Agricultural Water Management 284 (2023) 108345

Contents lists available at ScienceDirect

Agricultural Water Management

journal homepage: www.elsevier.com/locate/agwat

Sustainable irrigation management in tropical lowland rice in Brazil

Victor Meriguetti Pinto [a,*], Andre Froes de Borja Reis [b], Marina Luciana Abreu de Melo [a], Klaus Reichardt [a], Deivison Santos [c], Quirijn de Jong van Lier [a]

[a] Center for Nuclear Energy in Agriculture (CENA/USP), Piracicaba, São Paulo, Brazil
[b] Agricultural Center, Louisiana State University, Alexandria, LA, USA
[c] Embrapa Fisheries and Aquaculture (EMBRAPA), Palmas, Tocantins, Brazil

ARTICLE INFO

Handling Editor - Dr Z Xiying

Keywords:
Rice
Irrigation
Water productivity
SWAP model
Cerrado

ABSTRACT

Drought events and water use conflicts drive the need for more efficient water management in rice-growing areas of the Brazilian Cerrado. Recent studies have shown the advantages of adopting water-saving irrigation in the region but a comprehensive assessment is needed. This study aims to model the performance of rice cultivation and water productivity in the tropical floodplains of the Cerrado biome of northern Brazil in response to irrigation management under contrasting seasonal rainfall levels. Twenty-seven scenarios of rice cultivation, resulting from the combination of three sites, three irrigation treatments, and three rainfall regimes, were simulated with the calibrated and validated hydrological model SWAP/WOFOST. The rainfall levels high (1501 mm), intermediate (952 mm), and low (510 mm) were relative to 120 days and obtained from weather stations located in the region. Two irrigation methods (flooding and water-saving irrigation) were compared against rainfed cultivation. Actual transpiration of the flooding and water-saving irrigation was 9 % and 4 % higher in the intermediate and high rainfall scenarios while it was 30 % and 20 % higher in the low rainfall scenario compared to the rainfed treatment. The largest deep percolation loss was 12700 mm per season for flood irrigation in the low rainfall scenario, whereas the lowest one was 349 mm for the rainfed treatment in the low rainfall scenario. Changing from flooding to water-saving irrigation increases water productivity by an average of 9 % and decreases relative grain yield by 5–12 %. Water productivity based on bottom flux increased on average by about five times (high rainfall scenario) to ten times (low rainfall scenario) when comparing flooding with water-saving irrigation. Results suggest that saving irrigation based on crop transpiration can reduce deep percolation losses and increase water productivity in the rice-growing areas of the Brazilian Cerrado.

1. Introduction

Rice is one of the most produced commodities in Brazil (over 10 Mt in 2021/22), with 92 % of the production coming from lowland irrigated agrosystems (CONAB, 2022). The country's largest rice cultivation area is located in the subtropical lowlands in South Brazil, which account for 83 % of the national annual production. Farmers in South Brazil employ the traditional method of continuously flooding fields throughout the crop season, which is also the most practiced strategy worldwide [e.g., California Valley (Perry et al., 2022), Mekong Delta (Tong, 2017), Indo Gangetic Plain (Choudhury and Singh, 2016)]. Rice is the staple food in South America, and due to the increasing demand for its consumption, rice cultivation in Brazil has expanded to new agricultural areas since the early 2000s (Fig. 1). Many growers employ the management practices such as continuous flooding suited to the traditional regions in these new areas without having proof of whether they are the best option, whereas continuous flooding may often lead to productivity losses or overusing of natural resources.

Water ponding occurs on top of the soil surface when rainfall or irrigation intensity exceeds soil infiltration capacity. Water management and use in flood irrigation are highly sensitive to soil hydraulics and internal drainage characteristics. Lowland Cerrado soils do not present the typical dense and impermeable layer below the root zone that restricts water percolation in traditional rice-growing regions (Bouldin, 1986) but may contain plinthite and a textural gradient that reduces water infiltration rate and helps to keep the soil water content near-saturation (Embrapa, 2008). Depending on the soil attributes and the agricultural practices employed by the farmer, flood irrigation in the tropical floodplains of the Cerrado biome can demand a large amount of water. Up to 35 mm d^{-1} of water is needed to maintain the ponding

* Corresponding author.
E-mail address: meriguettiv@gmail.com (V.M. Pinto).

https://doi.org/10.1016/j.agwat.2023.108345
Received 12 July 2022; Received in revised form 6 December 2022; Accepted 1 May 2023
Available online 12 May 2023

layer in the flooding condition in tropical lowland soils (Embrapa, 2008), which is substantially higher than the requirements for sub-tropical soils - from 6 to 15 mm d^{-1} (SOSBAI, 2018). The rainfall regime affects the quantity of water needed for continuous flood irrigation. During the wet season, the water table level can be close to the soil surface in lowland Cerrado soils and its presence affects soil drainage. If the water table level is close to the soil surface, the drainage is poor, benefiting the formation of a ponding layer over the soil surface. Therefore, the suitability of using flood irrigation in the lowland areas of the Brazilian Cerrado needs a better evaluation focusing on the recommendation of sustainable irrigation management.

Irrigation strategies like shallow-wet irrigation, controlled irrigation (Zhuang et al., 2019), intermittent flooding, alternating wetting and drying (Carracelas et al., 2019; Yamaguchi et al., 2019), and irrigation based on soil water content or matric potential (Singh et al., 2021; Kadiyala et al., 2015; Kukal et al., 2005) are some of the alternatives to continuous flooding that can save water in lowland rice production. Wang et al. (2020) concluded that for rice paddies in China, alternating wetting and drying irrigation slightly benefited yield and reduced the amount of water needed. Zhuang et al. (2019) indicated that using controlled irrigation, in which surface water is maintained only in the "turning green" and the "early tillering" stages, had the highest average water-saving rate and the highest average pollutant reduction rate in paddy fields in China. Borja Reis et al. (2018a, 2018b) experimentally evaluated irrigation methods for rice cultivation in lowland areas of the Cerrado. They concluded the rainfed (aerobic) rice systems had equivalent or better crop performance and water productivity than other irrigation regimes. However, Borja Reis et al. (2018a, 2018b) did not consider different soils and climate scenarios. Few studies on rice irrigation have been carried out in the Brazilian tropical floodplains and, therefore, more investigations are needed to assess the rice performance response to the irrigation regime.

Field experiments can help analyze irrigation management concerning soil characteristics and rainfall regimes, but they are expensive and labor-intensive. Process-based simulation models such as SWAP (Kroes et al., 2017), DAISY (Hansen et al., 1990), and HYDRUS (Šimůnek et al., 2008) are recommended to evaluate scenarios in which it is necessary to obtain data in the short term and at a relatively low cost.

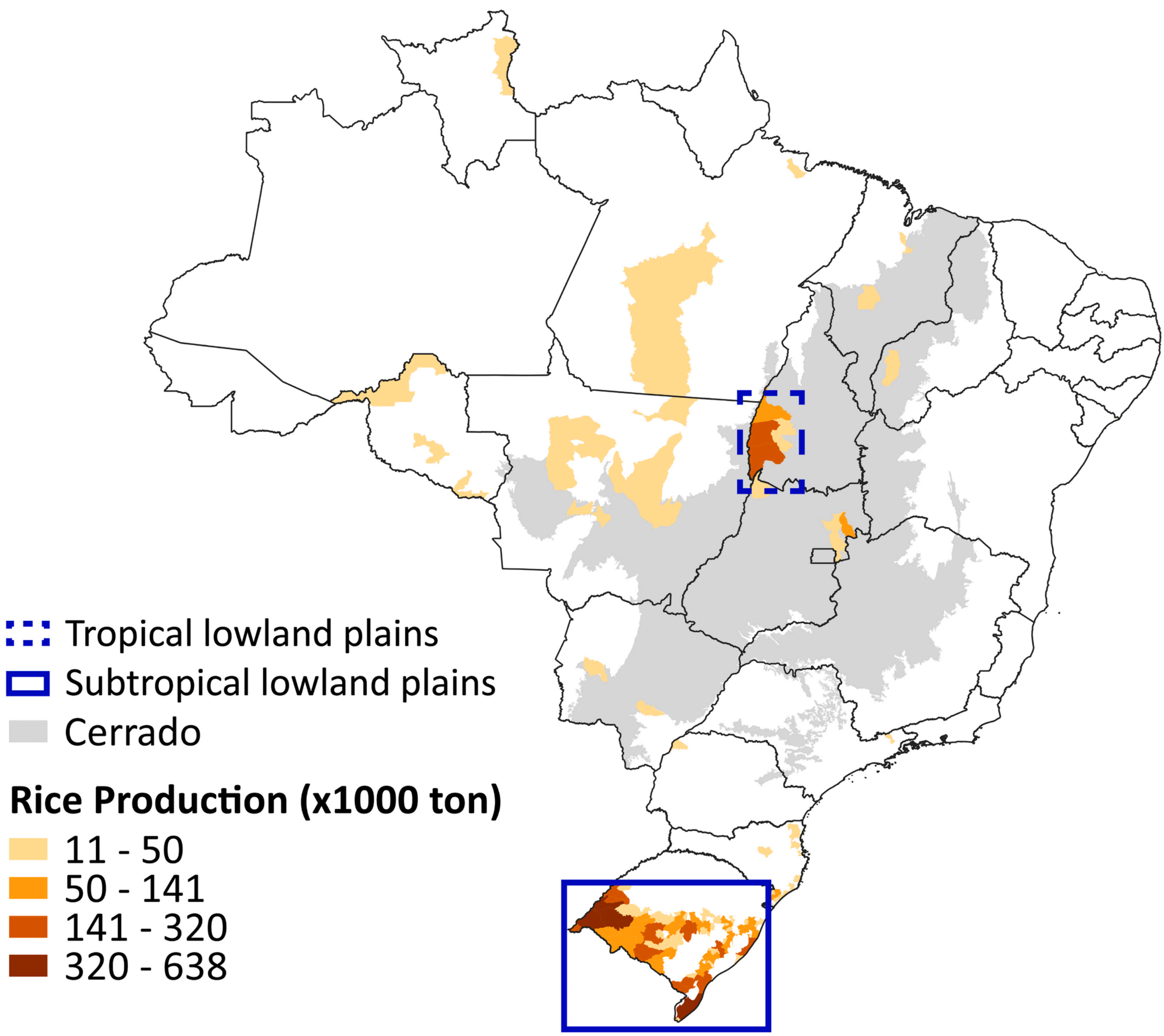

Fig. 1. Rice production (metric ton) in Brazil per municipality in 2020 (IBGE, 2022), traditional (subtropical lowland plains), and new (tropical lowland plains) rice-growing regions.

The SWAP model has been used in several agricultural research projects (Gelsinari et al., 2021; Bonfante et al., 2020; Ismail et al., 2020; Pinheiro et al., 2019; Yuan et al., 2019; Kroes et al., 2019; Taufik et al., 2018) and has shown its effectiveness in describing soil water dynamics and applicability to case studies of crop performance in Brazil (Melo and De Jong van Lier, 2021; Turek et al., 2020; Pinheiro et al., 2016; Durigon et al., 2012). The SWAP model contains the detailed crop growth routine WOFOST (De Wit et al., 2019) developed to simulate potential yields and water-limited yields and applied for over two decades as part of crop yield forecasting operating systems.

We hypothesize that conservative or water-saving irrigation methods could be employed to improve rice cultivation in the tropical floodplains of the Brazilian Cerrado area by significantly reducing the use of water with little or no yield penalties compared with traditional irrigation management (flood irrigation). In this context, we carried out model simulations to evaluate the performance of rice cultivation in these areas in response to flooding and water-saving irrigation treatments. Our objective was to assess soils with distinct hydraulic properties and cultivated with rice crops regarding water use and crop productivity under various rainfall and irrigation amounts.

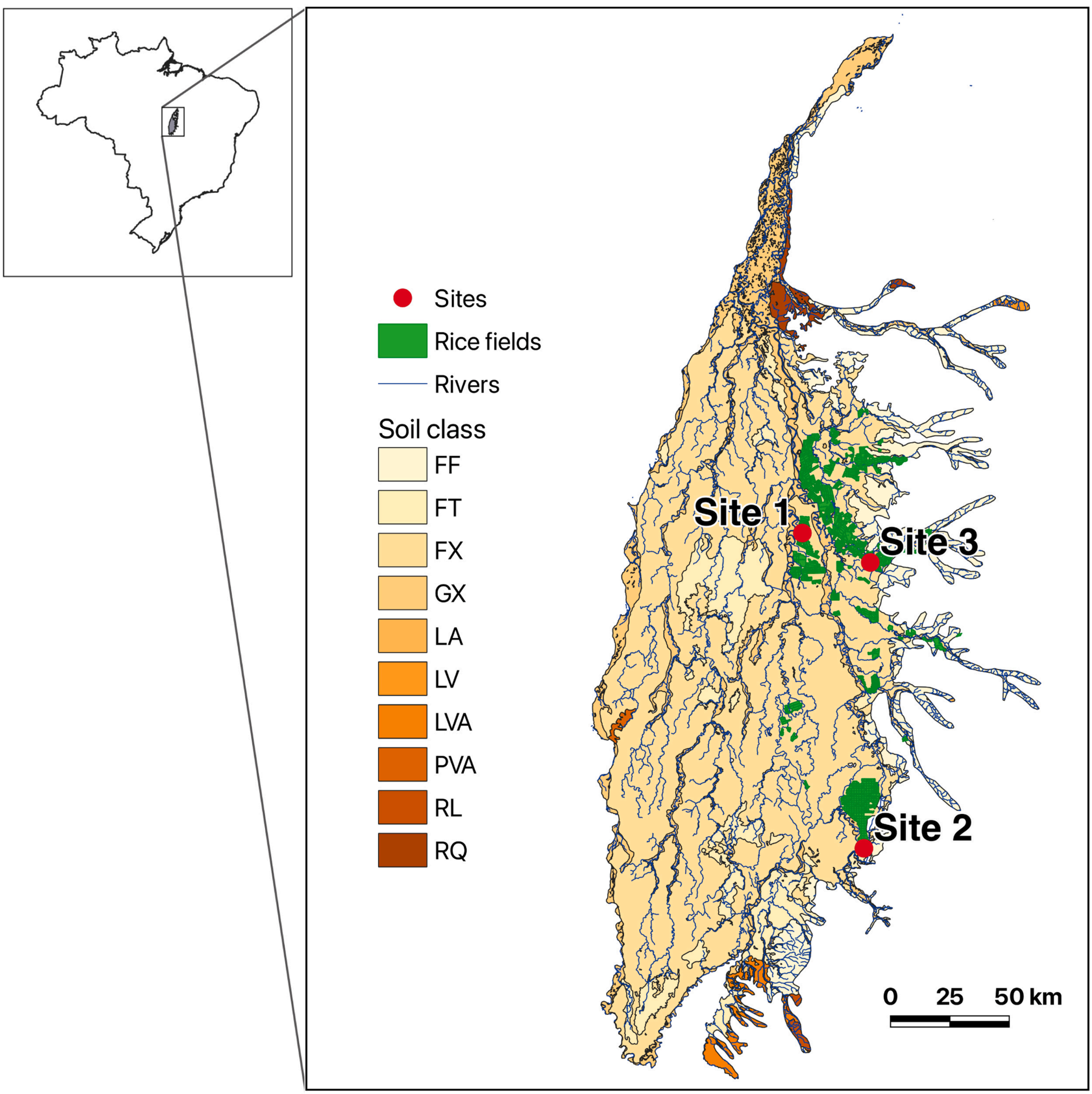

Fig. 2. Location of the soil sampling experimental sites (sites 1–3) on a soil map. Soil types use acronyms from the Brazilian Soil Classification System (Santos et al., 2018a, 2018b). Classes correspond to the WRB (FAO, 2006) Plinthosols (FF, FT, and FX), Gleysols (GX), Ferralsols (LA, LV, and LVA), Acrisols (PVA), Leptsols (RL), and Arenosols (RQ). The soils at sites 1, 2 and 3 are Plinthosols. Rice fields refer to the season 2019/2020.

2. Materials and methods

2.1. Experimental data

Experiments were carried out in the municipality of Lagoa da Confusão, State of Tocantins, in Northern Brazil (10°46′39.80″ S; 49°55′20.94″ W) during the years 2014, 2015, and 2016. Two seasons of rice cultivation were chosen for the experimental measurements: 1) Season 2014/2015, from November 18, 2014, to March 20, 2015; and 2) Season 2015/2016, from December 9, 2015, to April 7, 2016. See Borja Reis et al. (2018a, 2018b) for more information on the experimental design.

Three locations (site 1, Lagoa da Confusão 10°46′39.80″ S; 49°55′20.94″ W; site 2, Unitins 12°0′ S 49°41′ W; site 3, Urubu 10° 53′S 49° 39′ W) of different soil types were selected for soil sampling (Fig. 2). Undisturbed soil samples were taken from the soil layers 0–10, 10–20, 20–40, 40–90 cm in each of the three sites to determine the soil hydraulic parameters θ_s, θ_r, n and α (Table 1).

2.2. The SWAP hydrological model

2.2.1. Water flow and balance

The SWAP hydrological model (Kroes et al., 2017) is a Richards equation-based model that simulates water, solutes, and heat transport in the soil vadose zone. SWAP transport processes are predominantly vertical (one-dimensional), and the model simulations are at the field scale. The vertical domain of the model ranges from just above the canopy to the shallow groundwater.

The Richards equation in one dimension added by the sink terms S is implemented in SWAP to calculate the water movement in the soil matrix (Van Dam and Feddes, 2000) as follows:

$$C(h)\frac{\partial h}{\partial t} = \frac{\partial}{\partial z}\left[K(h)\left(\frac{\partial h}{\partial z}+1\right)\right] - S(h) \tag{1}$$

where C is the differential water capacity ($\partial\theta/\partial z$) (cm^{-1}), θ (cm^3 cm^{-3}) is the volumetric soil water content, t (d) is time, and S (cm^3 cm^{-3} d^{-1}) is the water extraction rate by plant roots. SWAP uses the Richards equation for describing water flux in the unsaturated and saturated zones of the soil and solves Eq. 1 numerically, using the relations between θ, h, and K, with the Mualem-Van Genuchten functions, θ(h) and K(h) (Mualem, 1976; Van Genuchten, 1980).

Table 1
Soil water retention parameters and saturated hydraulic conductivity of the three experimental sites.

Depth (cm)	θ_s (cm^3 cm^{-3})	θ_r (cm^3 cm^{-3})	n	α (cm^{-1})	K_s (cm d^{-1})
Site 1					
0–10	0.59	0.00	1.22	0.0049	54
10–20	0.51	0.00	1.25	0.0026	31
20–40	0.50	0.00	1.21	0.0014	19
40–90	0.44	0.00	1.28	0.0004	10
Site 2					
0–10	0.37	0.00	1.51	0.0002	13
10–20	0.40	0.00	1.54	0.0003	13
20–40	0.45	0.00	1.26	0.0012	17
40–90	0.43	0.00	1.26	0.0006	12
Site 3					
0–10	0.35	0.18	1.51	0.0050	14
10–20	0.35	0.00	1.25	0.0034	9
20–40	0.33	0.00	1.30	0.0020	12
40–90	0.36	0.00	2.06	0.0002	9

Note: θ_s, saturated soil water content; θ_r, residual soil water content; n and α, shape parameters of the soil water retention curve (Van Genuchten, 1980); K_s, saturated hydraulic conductivity.

2.2.2. Plant module

In this study, the detailed crop model available in SWAP was used to simulate crop growth performance in irrigated rice fields. The detailed crop module is an adaptation of the World Food Studies (WOFOST) model (Boogaard et al., 2014) and simulates absolute productivity. The prediction of potential production is determined by solar radiation, air temperature, CO_2 concentration in the atmosphere, crop characteristics, and planting date. It requires plant biometrics, CO_2 assimilation, dry matter partitioning data, and other crop information. SWAP-WOFOST simulates the reduction of potential crop productivity due to water, salinity, and nutrient deficit (Kroes et al., 2017). The transpiration reduction function of Feddes et al. (1978) rules the reduction in crop productivity due to water stress. Nutrient deficiencies and salinity were not considered limiting factors to crop performance.

2.2.3. Soil evaporation

Soil evaporation E (cm d^{-1}) is predicted in SWAP using the Penman-Monteith equation (Monteith, 1981). For wet soil or in ponded conditions, the actual soil evaporation simulated by SWAP equals the potential soil evaporation E_p. When the soil gets drier, the soil hydraulic conductivity decreases, and the evaporation is reduced to the actual evaporation rate (E_a) (Kroes et al., 2017). In SWAP, the maximum evaporation rate sustained by the topsoil, E_{max} (cm d^{-1}), is calculated according to Darcy's law (Eq. 2).

$$E_{max} = -K_{1/2}\left(\frac{h_{atm} - h_1 - z_1}{z_1}\right) \tag{2}$$

where $K_{1/2}$ is the average hydraulic conductivity (cm d^{-1}) between the soil surface (h_{atm}) and the first soil compartment (h_1) in SWAP, h_{atm} is the soil pressure head (cm) in equilibrium with the air relative humidity, h_1 is the soil water pressure head of the first soil compartment, and z_1 is the depth (cm) at the middle of the first soil compartment. h_{atm} is initially equal to $-2.75 \cdot 10^5$ cm in SWAP and is updated according to the atmospheric and soil water conditions. z_1 is automatically calculated according to the soil compartments chosen by the model user.

2.2.4. Bottom boundary condition

The free drainage bottom boundary condition was used in this study. In this lower boundary condition, water is considered to move vertically by gravity alone, under a unit hydraulic head ($\partial H/\partial z$) gradient. Consequently, a bottom flux (q_{bot}) equal to the saturated hydraulic conductivity of the lowest soil compartment (K_{lc}) is established:

$$\frac{\partial H}{\partial z} = \frac{\partial z}{\partial z} = 1 \tag{3}$$

$$q_{bot} = -K_{lc} \tag{4}$$

Eq. (3) indicates that only the gravity potential influences the soil water movement in the bottom of the soil profile, i.e., the hydraulic head H equals z ($\partial H/\partial z = 1$). Eq. (4) is the Darcy equation for water flux considering water moves only with the gravitational potential.

2.3. Data input

Soil water retention curves were obtained by measuring the soil water content after submitting soil samples to pressure heads of −10, −20, −60, −330, −1000, −3000, and −15,000 cm in porous plate pressure chambers. The Van Genuchten (1980) model was fitted to θ-h data pairs for each of the four sampled soil layers using the RETC software (Van Genuchten et al., 1991). RETC generates the means, standard deviations, and the correlation matrix of the Van Genuchten parameters θ_s, θ_r, α, and n. Table 1 shows the mean values of the Van Genuchten parameters for the three sites and four analyzed depths. Fig. 3 shows the mean retention curves of the three study sites, in which each curve was built with the mean of θ-h pairs obtained for the four depths. Saturated

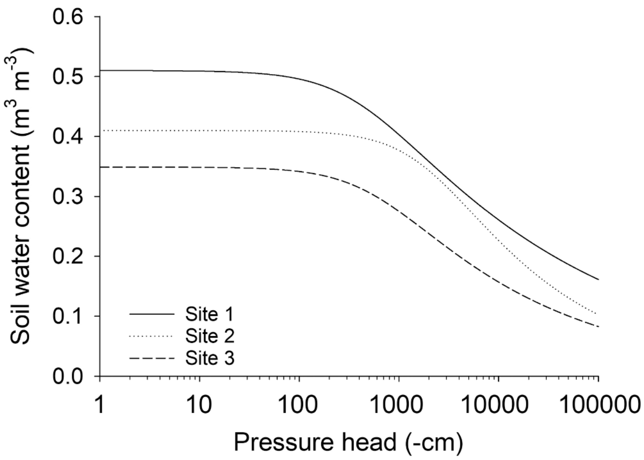

Fig. 3. Soil water retention curves of the three study sites. Each curve was built with the mean of θ-*h* pairs obtained for the four analyzed depths. Soils at all three sites are classified as Plinthosols.

hydraulic conductivity K_s (Table 1) was obtained by Neural Network Analysis (Rosetta software, v. 1.1) using soil texture, dry bulk density (complementary material), and water content at pressure heads of − 330 cm and − 15,000 cm as inputs. Most SWAP crop-file parameters (Table 2) were taken from the WOFOST data set online (De Wit, 2022).

Table 2
Plant parameters used in the simulation with SWAP-WOFOST.

Description	Parameter	Rice	Unit
Plant factor (maximum value)	CF_{max}	1.20	cm
Temperature sum from emergence to anthesis	T_{sumea}	1250*	°C
Temperature sum from anthesis to maturity	T_{sumam}	690*	°C
CO_2 assimilation rate (maximum value)	$A_{max,d}$	47	kg ha^{-1} h^{-1}
Extinction coefficient for diffuse visible light	k_{dif}	0.40	-
Extinction coefficient for direct visible light	k_{dir}	0.75	-
Light use efficiency	ε	0.48*	kg ha^{-1} h^{-1} J^{-1}/J m^2 s^{-1}
Efficiency of conversion into leaves	C_{vl}	0.78	kg kg^{-1}
Efficiency of conversion into storage organs	C_{vo}	0.79	kg kg^{-1}
Efficiency of conversion into roots	C_{vr}	0.72	kg kg^{-1}
Efficiency of conversion into stems	C_{vs}	0.69	kg kg^{-1}
Relative increase in respiration rate with temperature	R_{it}	2.00	kg CH_2O kg^{-1} d^{-1}
Relative maintenance respiration rate of leaves	R_{ml}	0.03	kg CH_2O kg^{-1} d^{-1}
Relative maintenance respiration rate of storage organs	R_{mo}	0.002	kg CH_2O kg^{-1} d^{-1}
Relative maintenance respiration rate of roots	R_{mr}	0.010	kg CH_2O kg^{-1} d^{-1}
Relative maintenance respiration rate of stems	R_{ms}	0.015	kg CH_2O kg^{-1} d^{-1}
Relative death rate of leaves due to water stress (maximum value)	P_{dl}	0.03	d^{-1}
Critical pressure heads**	h_1	100	cm
	$h_{2\,u}$	55	cm
	$h_{2\,l}$	55	cm
	$h_{3\,h}$	-460	cm
	$h_{3\,l}$	-530	cm
	h_4	-16000	cm
Interception coefficient	a	0.25	cm
Root depth (maximum value)	$R_{rd,m}$	35	cm

* Parameters fitted during calibration.
** $h_{3\,h}$ and $h_{3\,l}$ were obtained from the experimental measures presented in Santos et al. (2018a, 2018b). h_4 was set according to Singh et al. (2006).

2.4. Model calibration and validation

Two datasets of experimentally obtained values of field water content θ (Borja Reis et al., 2018a, 2018b) were used to evaluate model performance. The first dataset refers to θ values measured with six replicates between December 1 and December 20, 2014; the second data set refers to θ measurements with two replicates between January 20 and April 7, 2016. The first dataset corresponds to irrigation methods employed in the studies of Borja Reis et al. (2018a, 2018b). Only the interval of rainfed rice cultivation (the first 25 days of cultivation approximately) was considered for model calibration in the 2014/2015 season because SWAP requires daily irrigation quantities for simulations. Such data were not available in the studies of Borja Reis et al. (2018a, 2018b). The second dataset consists of continuous measurements of θ in two different plots of rainfed rice cultivation in the 2015/2016 season and was used to validate the model.

A few crop parameters were selected to be fitted manually in the calibration step of the crop module of SWAP (WOFOST). The calibrated parameters were the temperature sum required to complete the vegetative stage (T_{sumea}), the temperature sum needed to complete the reproductive stage (T_{sumam}), and the light use efficiency (ε). Data of leaf area index (*LAI*), aboveground biomass (*AGB*), and soil water content (θ) measured experimentally at site 1 with no irrigation during the 2014/2015 season were used to assess the effectiveness of the model to simulate *LAI*, *AGB*, and θ in the calibration step. The simulated values were compared with experimentally obtained values during the season 2015/2016 in the validation procedure of the model.

Stochastic simulations with SWAP were performed to obtain the confidence interval in which the experimental values of θ should be situated and to determine the quality of the simulations. The means, standard deviations, and the correlation matrix of the soil hydraulic parameters obtained from the fit of the experimental θ-*h* pairs to the Van Genuchten model generated a dataset of ten thousand (10,000) realizations of θ_s, α, and *n* for each soil type and soil layer. Stochastic realizations of the Van Genuchten parameters were obtained using the Cholesky decomposition technique (Pinheiro and De Jong van Lier, 2021), considering the correlation matrix between soil hydraulic parameters. Each generated realization of the parameters θ_s, α, and *n* was used in SWAP to simulate a complete rice cultivation season. As a result, 10,000 simulated values of θ were obtained for each day of the rice season. The 5th, 50th, and 95th percentiles were selected from these θ values, and an interval of θ data was created, representing the most probable results of θ for the two simulated scenarios (seasons 2014/2015 and 2015/2016). The 5th, 50th, and 95th percentiles limits for the simulated θ validated the model simulations.

2.5. Statistical analysis

The Root Mean Square Error RMSE (Eq. 5), the index of agreement d (Eq. 6), and the Nash-Sutcliff model efficiency NSE (Eq. 7) were used for quantifying the quality of the model calibration and validation.

$$\mathrm{RMSE} = \sqrt{\frac{\sum_{i=1}^{n}(P-O)^2}{n}} \tag{5}$$

$$\mathrm{d} = 1 - \frac{\sum_{i=1}^{n}(P-O)^2}{\sum_{i=1}^{n}(|P-O|+|O-\overline{O}|)} \tag{6}$$

$$\mathrm{NSE} = 1 - \frac{\sum_{i=1}^{n}(P-O)^2}{\sum_{i=1}^{n}(O-\overline{O})^2} \tag{7}$$

where *n* is the number of values used for the calculations, *P* is the soil water content θ predicted by SWAP, *O* is the θ measured experimentally, and $\overline{O}$ is the average of the measured θ values.

The 50th percentile of the stochastic simulation was used for calculating the RMSE, d, and NSE. The RMSE is the standard deviation of the residuals and measures how spread-out these deviations are. RMSE has the same unit of measurement of the variable from which the residuals are calculated. The index d measures the agreement of the model simulations to the experimental values. The dimensionless d has a minimum value of 0, indicating no concordance, and a maximum of 1, indicating a perfect agreement. NSE is also dimensionless, and it can assume values between -∞ and 1. NSE equal to 1 means the model perfectly fits the experimental values, and an NSE lower than 0 means that the average of the experimental observations is a better prediction than the model prediction (Groenendijk et al., 2014).

2.6. Simulation scenarios

Twenty-seven scenarios of rice cultivation, resulting from the combination of three soil types (Table 1), three irrigation treatments, and three rainfall regimes, were evaluated with the calibrated and validated SWAP/WOFOST model. The simulated treatments were:

1. Rainfed: no irrigation, only rainfall;
2. Water-saving irrigation (back to field capacity irrigation), in which the model adds water automatically to the system to return the soil water storage to field capacity ($h = -100$ cm) every time the relative transpiration falls below 95 %;
3. Flood irrigation: daily irrigation maintains a water layer of 6 cm over the soil surface during the cropping season, simulating the flooding conditions of the field experiment.

Rainfall regimes were obtained from weather stations located in the State of Tocantins, Brazil. Each rainfall amount was relative to periods of 120 days, from November to April, between 2006 and 2020. The rainfall amounts selected for the simulations were 1501 mm, 952 mm, and 510 mm, and correspond to high (maximum), intermediate (median), and low (minimum) rainfall scenarios, respectively.

2.7. Relative grain yield

Relative grain yield Y_r (%) is the ratio between the simulated actual grain yield Y_a and potential grain yield Y_p. The simulated rice Y_a is affected by water availability from rainfall and irrigation and water scarcity. In its term, Y_p is only affected by the radiation fluxes above the canopy, air temperature, and crop partitioning factors responsible for dry matter partitioning and growth respiration (Kroes et al., 2017).

2.8. Water productivity

Water productivity WP (kg m^{-3}), in general terms, is the rate of dry matter produced per unit volume of water used. Grain yield can be used instead of dry matter production. The amount of water used can be replaced by crop transpiration, the sum of evaporation and crop transpiration, or even the sum of rainfall and irrigation amounts (Vazifedoust et al., 2008). In this study, water productivity is:

i) the ratio of the simulated grain yield Y and transpiration T (Eq. 8):

$$WP_T = \frac{Y}{T} \tag{8}$$

ii) the ratio of measured grain yield Y and evapotranspiration ET (Eq. 9):

$$WP_{ET} = \frac{Y}{ET} \tag{9}$$

iii) the ratio of simulated grain yield and evapotranspiration ET and bottom water flux Q, i.e., deep percolation loss per season (Eq. 10):

$$WP_{ETQ} = \frac{Y}{ETQ} \tag{10}$$

Eq. 8 provides the physiological performance of the crop and is related to the diffusion rates of CO_2 and H_2O molecules through the stomata. Eq. 9 and Eq. 10 consider the loss of water by evaporation and by deep percolation, respectively.

3. Results and discussion

3.1. Model calibration and validation

Fig. 4 shows the results of soil water content (θ) obtained experimentally and simulated by SWAP for two intervals of rainfed rice cultivation at site 1. The peaks in θ correspond to the rainfall events, some of which reached more than 100 mm in one day. The θ peaks are more frequent in the 2015/2016 season (Fig. 4B), whereas the θ observed remains relatively constant in the 2014/2015 season (Fig. 4 A). Due to the constancy of the average θ obtained experimentally in the 2014/2015 season (Fig. 4 A), the average of observed θ was a better predictor than the model during this interval (NSE < 0). Nonetheless, most of the observed θ is within the p5 and p90 limits (percentiles 5 and 90, respectively). In contrast, RMSE and d indexes for the

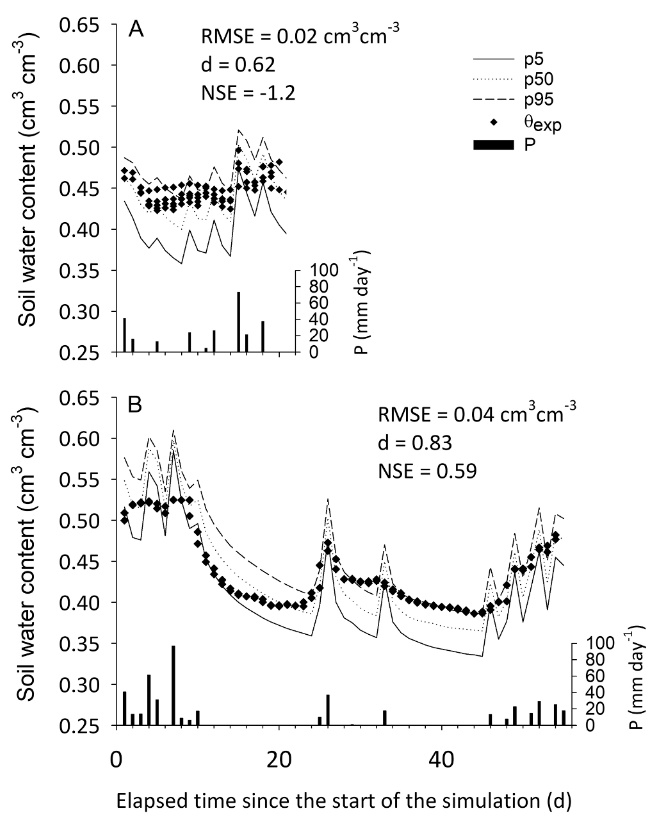

Fig. 4. Soil water content (θ) simulated (percentiles p5, p50, and p95) and measured experimentally (markers) by Borja Reis et al. (2018b) during seasons 2014/2015 (A) and 2015/2016 (B), together with daily rainfall amount (P). p50, the 50th percentile (median); p5, the 5th percentile; and p95, the 95th percentile of the θ values simulated with the SWAP model. RMSE is the root mean square error, d is the index of agreement, and NSE is the Nash-Sutcliff model efficiency index.

2015/2016 season showed satisfactory model performance during this simulated period. The statistical indexes RMSE, d, and NSE of the 2015/2016 season confirm the agreement of θ simulations with experimental data.

Fig. 5 A and Fig. 5 C show the results of leaf area index (*LAI*) and aboveground biomass (*AGB*) simulated with SWAP after calibration of plant parameters. Fig. 5B and Fig. 5D show the results of the same variables after model validation. *LAI* and *AGB* simulations show that SWAP simulations effectively predicted the plant performance in both cycles. Rice grain yield simulated with SWAP/WOFOST was 9030 kg ha^{-1} in 2014/2015 and 7135 kg ha^{-1} in 2015/2016. Grain yield amounts obtained experimentally were 10576 kg ha^{-1} and 8531 kg ha^{-1}, respectively, for seasons 2014/2015 and 2015/2016. The differences between simulated and observed grain yield may be because SWAP does not include any effect of suboptimal soil fertility, which may have had some effect on rice growth.

3.2. Simulation scenarios

3.2.1. Water balance

The water balance components for all irrigation treatments and soil combinations are shown in Fig. 6. In the water-saving treatments, the highest irrigation amount was 754 mm for site 3 in the low rainfall scenario, and the lowest one was 46 mm for site 2 during the high rainfall scenario. The highest irrigation amount applied in flooding was 12754 mm (106 mm d^{-1}) for site 2 in the low rainfall scenario, and the lowest one was 8247 mm (69 mm d^{-1}) for site 3 in the high rainfall scenario. The smallest water amount used in flood irrigation was 10 times higher than the largest amount used in water-saving irrigation treatments.

The highest deep percolation loss per season (Q) within the water-saving irrigation treatments was 2063 mm (site 3) in the high rainfall scenario; within the flood irrigation treatments, the highest Q was 12675 mm (site 2) in the low rainfall scenario. The lowest Q was 349 mm for the rainfed treatment at site 2 in the low rainfall scenario, which is very close to Q for site 1 with no irrigation and low rainfall conditions (Fig. 6). The Q values obtained in this study were larger than those measured experimentally in traditional rice fields. LaHue and Linquist (2021) obtained percolation rates for Californian rice fields from 0.04 to 69.5 mm per season and an average of 1306 mm total water input (rainfall + irrigation). Castañeda et al. (2002) measured a percolation of 128 mm in rice fields cultivated in the Philippines during the dry season and 68 mm during the wet season, being the total water input of 1370 and 1325 mm, respectively.

As no experimental data on the groundwater level (*GWL*) were available, the lower boundary condition used in SWAP was free drainage, i.e., the bottom water flux was considered equal to the soil saturated hydraulic conductivity of the lowest soil compartment (Section 2). Using this boundary condition, the *GWL* is simulated and modulated by rainfall, infiltration rate, and the hydraulic conductivity of the bottom compartment. In our simulations, the *GWL* stayed below the rooting depth (around 1 m) for most of the simulated period, coming close to the soil surface only for a few days after high-intensity rain events. The detachment of the *GWL* from the vadose zone or even the soil surface may be the reason for the high values of Q obtained in flood irrigation treatments. Additionally, SWAP simulated only vertical soil water fluxes. A relatively small lateral seepage may have occurred in flooded rice fields (LaHue and Linquist, 2019), but this study does not consider lateral flow.

The average increases in T_a during the intermediate and high rainfall scenarios were 9 % and 4 % when comparing the results for actual transpiration (T_a) of the flood and water-saving irrigation treatments with the rainfed treatment (Fig. 6). When the flood irrigation was applied in the low rainfall scenario, T_a increased by 30 % on average

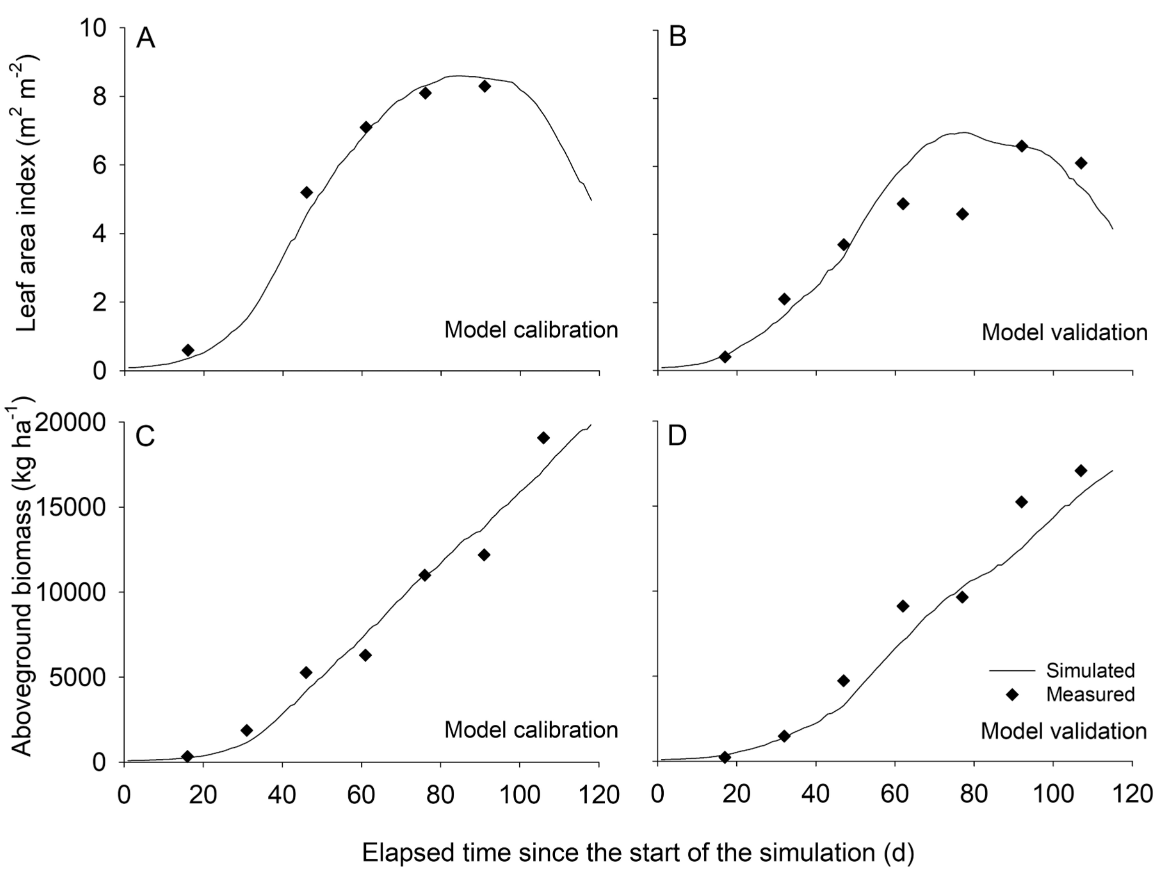

Fig. 5. Leaf area index (*LAI*) and aboveground biomass (*AGB*) simulated and measured during the 2014/2015 season (A and C) and the 2015/2016 season (B and D).

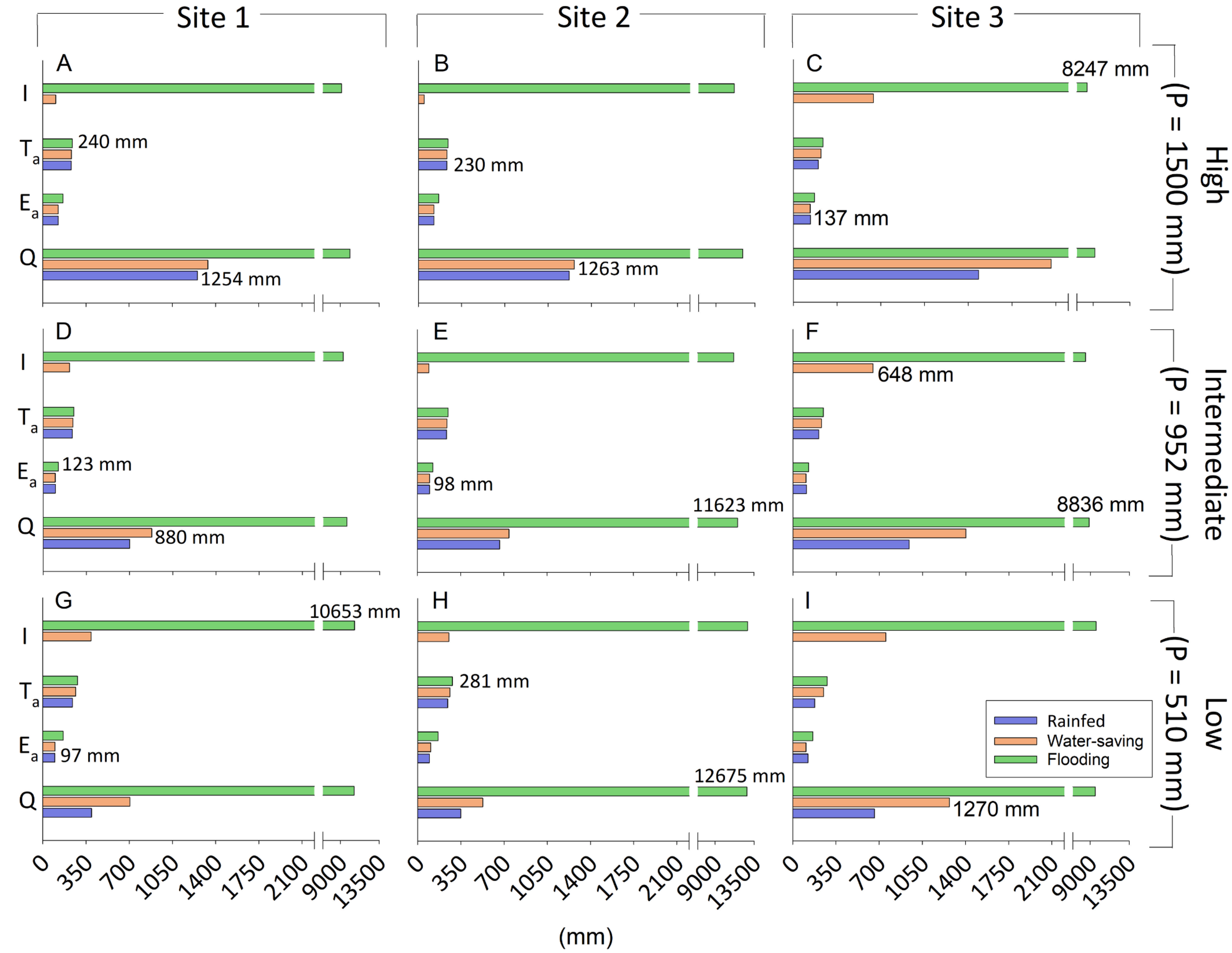

Fig. 6. Main components of the water balance calculated for rice cultivated at three sites under three rainfall regimes [A), B), and C): high; D), E), and F): intermediate; G), H), and I): low] and three irrigation treatments [rainfed (blue), water-saving (orange), and flooding (green)]. *I*, irrigation; T_a, plant transpiration; E_a, soil evaporation; *Q*, deep percolation loss.

compared with T_a obtained in the rainfed treatment. When water-saving irrigation was used in the low rainfall scenario, T_a increased by 20 % compared with the rainfed treatment. Therefore, irrigation is shown to be needed in the low rainfall scenario to maintain crop transpiration and optimize yield.

At site 3, significant increases in T_a were observed comparing the flood irrigation with the rainfed treatment. The increase in T_a was 57 % for the low rainfall scenario and 18 % for the high and the intermediate rainfall scenarios. The soil water retention curve at site 3 may explain the elevated sensitivity of T_a to irrigation. This soil has the lowest water storage capacity among the studied soils (Fig. 3). Since the soil water availability is even lower in the dry season (low rainfall), the water available to plants will be more limited than in other soils with greater water storage capacity. With a continuous water supply, e.g., under flood irrigation, water is available all the time and water storage capacity does not affect the transpiration which will be potential.

Soil evaporation E_a increased when the flood irrigation was used compared with the rainfed and the water-saving irrigation treatments (Fig. 6). At site 2, E_a increased from 95 mm (rainfed) to 165 mm (flood irrigation) in the low rainfall scenario. The lowest E_a increment occurred at site 3, from 110 mm (rainfed) to 126 mm (flood irrigation) in the intermediate rainfall scenario. E_a in flooded rice is expected to be high, almost equal to a free water surface. At site 3, E_a decreased from 125 mm (rainfed) to 108 mm (water-saving irrigation) in the low rainfall scenario. Such a decrease in soil evaporation is related to the higher soil cover by crop canopy in water-saving irrigation compared to the rainfed treatment.

3.2.2. *Grain yield and water productivity*

Most of the simulated grain yields for the rainfed treatment were significantly lower than the potential grain yield in the low rainfall scenario (Fig. 7). The water-saving irrigation treatment did not significantly increase the relative grain yield (Y_r) compared with the rainfed treatment in the low rainfall scenario for the three sites. The Y_r of the water-saving irrigation in the low rainfall scenario was at most (at site 1) 3 % higher than the grain yield in the rainfed treatment. The flood irrigation treatment increased Y_r from 8 % (site 2) to 25 % (site 3) compared with other treatments in the low rainfall scenario (Fig. 7). Grain yields simulated for site 1 and site 2 were similar to potential grain yields (Y_r between 94 % and 99 %) with or without irrigation for the intermediate and high rainfall scenarios. Based on these results, irrigation appears to be unnecessary in years with intermediate or high-rainfall amounts. Nevertheless, flood irrigation would increase grain yields for at least one of the sites (site 3) in years with low rainfall.

Regarding water use efficiency, Fig. 8A shows water productivity considering only transpiration, WP_T, Fig. 8B presents water productivity

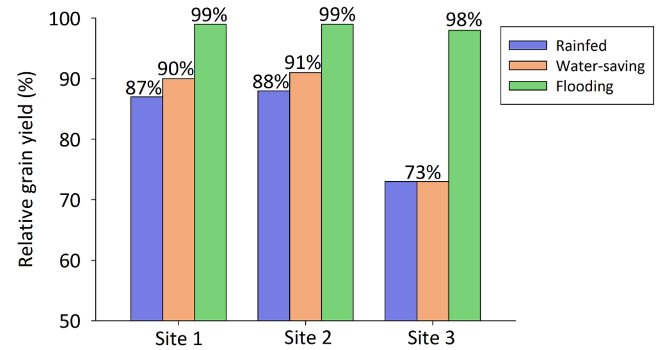

Fig. 7. Relative grain yield (Y_r) for three sites and three irrigation treatments with the low rainfall amount scenario (510 mm). Rainfed (blue): no irrigation; Water-saving (orange): irrigation back to field capacity every time the relative transpiration (T_a/T_p ratio) falls below 95 %; Flooding (green): permanent flood irrigation.

based on evapotranspiration, WP_{ET}, and Fig. 8C shows water productivity based on the sum of evapotranspiration and deep percolation, WP_{ETQ}. Simulations with low rainfall and rainfed treatment resulted in the highest WP_T values (from 3.7 to 4.2 kg m^{-3}) (Fig. 8A), WP_{ET} values (from 2.5 to 2.7 kg m^{-3}) (Fig. 8B), and WP_{ETQ} values (from 0.8 to 1.3 kg m^{-3}) (Fig. 8 C). There was no difference between WP_T obtained for the rainfed and the irrigation treatments, and there is no apparent tendency in the values of WP_T concerning the rainfall amounts (Fig. 8A). Most WP_{ET} values were in the range of 2.0 and 2.5 kg m^{-3}, and only three WP_{ET} values were in the range of 2.5 and 3.0 kg m^{-3} (Fig. 8B), which referred to the rainfed and water-saving irrigation treatments in the low rainfall scenario. Water demand from flood irrigation is evidenced in the water productivity indexes calculated as WP_{ET} and WP_{ETQ}. These indexes consider soil evaporation and deep percolation (Q), respectively, to estimate water productivity besides crop transpiration. WP_{ETQ} values are mainly influenced by Q, and that is why the lowest values of WP_{ETQ} were obtained in most of the high rainfall scenarios and for all scenarios with flood irrigation (Fig. 8C). WP_{ETQ} of flood irrigation treatment was 250 % lower than the second lowest WP_{ETQ}, which refers to water-saving irrigation in the high rainfall scenario at site 3.

WP_{ET} values agree with those calculated from field experiments in tropical floodplains of the Cerrado biome in Brazil (Borja Reis et al., 2018a, 2018b). However, WP_{ET} values obtained in this study were higher than values commonly obtained for irrigated rice, which are between 0.4 and 1.6 kg m^{-3} (Zwart and Bastiaanssen; , 2004; Tuong and Bouman, 2003; Dossou-Yovo and Saito, 2022). However, Mainuddin et al. (2020) reported average WP_{ET} values of 1.60 kg m^{-1} and 1.78 kg m^{-3} in two years, with the maximum reaching around 3.0 kg m^{-3}. WP_{ETQ} values obtained in this study are also similar to WP values reported by Singh et al. (2006) for rice crops in India.

An ideal irrigation management should result in high crop productivity with optimal water use recommended by a combined assessment of water productivity and grain yield. From our results, changing from flood irrigation to water-saving irrigation or rainfed treatment increases WP_{ET} and WP_{ETQ}, while the relative grain yield is little affected as a function of irrigation treatment for two of the three evaluated sites (Fig. 9). Flood irrigation treatment resulted in large deep percolation losses, which explains why WP_{ETQ} is significantly affected by changing from flooding to water-saving or rainfed treatments. Rainfed treatment showed that the grain yield is reduced considerably (23 %) at site 3 when the rainfall amount is low. However, water-saving irrigation increased WP_{ET} and WP_{ETQ} while grain yield was reduced by 13 %, which is almost half of the Y_r reduction when changing from flood irrigation to rainfed treatment. Therefore, from a combined assessment of grain yield and water use efficiency, water-saving irrigation is a promising method for rice cultivation in the lowland region of Cerrado, Brazil.

4. Conclusion

In the tropical floodplains of the Brazilian Cerrado, flood irrigation results in the highest grain yields but the lowest water use efficiency. This irrigation method is only recommended when rainfall is very low (below 500 mm per season) and if maximization of grain yield is preferable over water use efficiency. Choosing the water-saving irrigation method rather than the flood irrigation method increases water productivity by about 10 % and penalizes the rice grain yield by 5–13 %. Hence, as an alternative to the traditional method of flood irrigation employed in South Brazil, a more sustainable irrigation method based on crop transpiration is recommended for increasing the water use efficiency of rice production in Northern Brazil.

Declaration of Competing Interest

The authors declare the following financial interests/personal relationships which may be considered as potential competing interests: Victor Meriguetti Pinto reports financial support was provided by The Coordination for the Improvement of Higher Education Personnel.

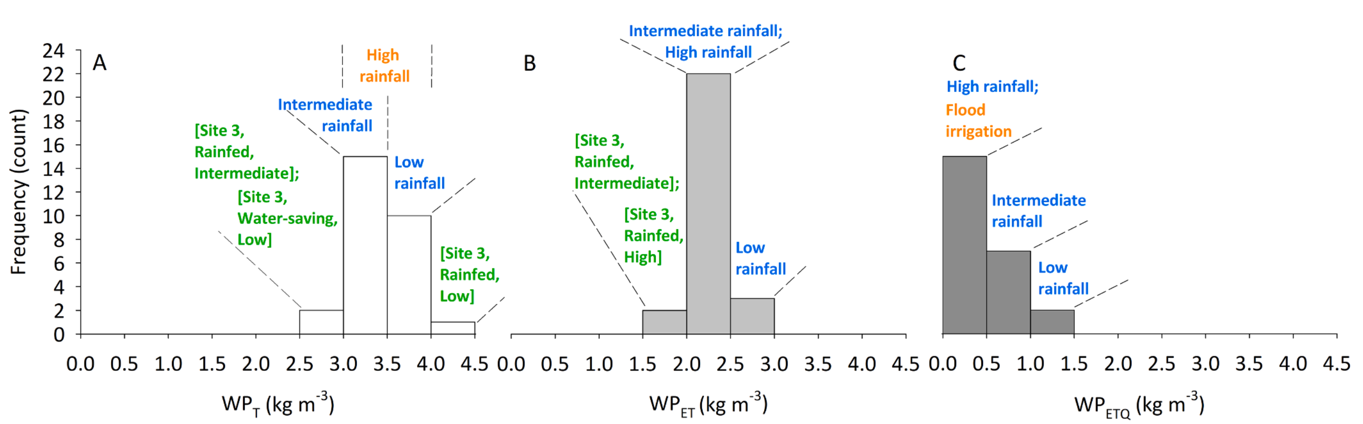

Fig. 8. Frequency of water productivity among 27 evaluated scenarios. A) WP_T, kg of grains per m^3 of transpiration; B) WP_{ET}, kg of grains per m^3 of evapotranspiration; and C) WP_{ETQ}, kg of grains per m^3 of evapotranspiration and deep percolation. Scenarios in orange indicate that all scenarios have WP values inside that range; scenarios in blue mean that most of the scenarios mentioned have WP values inside that range; scenarios in green designate a single combination of location (site), irrigation treatment, and rainfall amount.

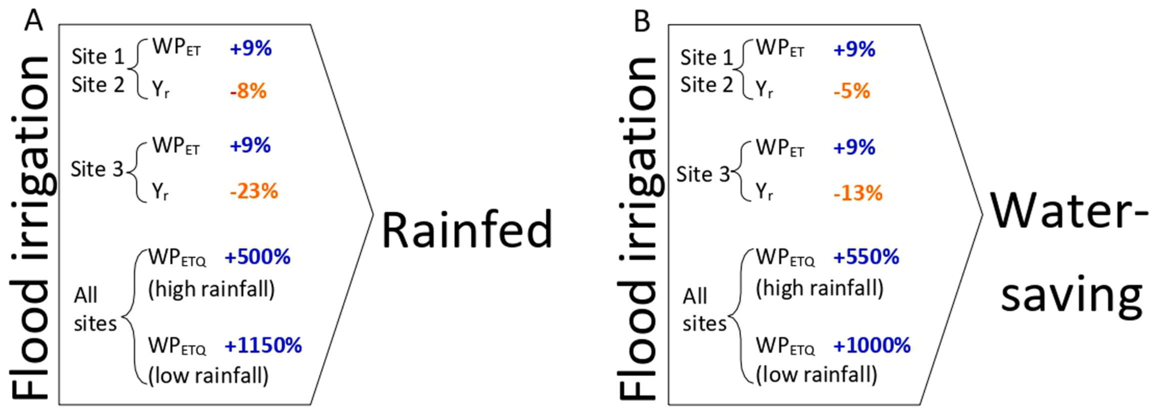

Fig. 9. Variation in water productivity (WP_{ET} and WP_{ETQ}) and relative grain yield (Y_r) when changing from flood irrigation to rainfed cultivation (A), and flood irrigation to water-saving irrigation (B). Variations in WP_{ET} and Y_r of site 1 and site 2 are averages of the results obtained in both sites. Increments in WP_{ETQ} are averages of the results obtained in all three sites.

Data availability

Data will be made available on request.

Acknowledgements

The authors are grateful to The Coordination for the Improvement of Higher Education Personnel (CAPES/ANA - DPB - FOMENTO CAPES, call #16/2017, Process #88887.636454/2021-00) for financial support.

Appendix A. Supporting information

Supplementary data associated with this article can be found in the online version at doi:10.1016/j.agwat.2023.108345.

References

Bonfante, A., Basile, A., Bouma, J., 2020. Exploring the effect of varying soil organic matter contents on current and future moisture supply capacities of six Italian soils. Geoderma 361, 114079. https://doi.org/10.1016/j.geoderma.2019.114079.

Boogaard, H.L., De Wit, A.J.W., Roller, J.A., Van Diepen, C.A., 2014. Wofost Control Centre 2.1; User's Guide for the Wofost Control Centre 2.1 and the Crop Growth Simulation Model WOFOST 7.1.7. Alterra, Wageningen University & Research Centre,, Wageningen (Netherlands).

Borja Reis, A.F., Almeida, R.E., Lago, B.C., Trivelin, P.C., Linquist, B., Favarin, J.L., 2018a. Aerobic rice system improves water productivity, nitrogen recovery and crop performance in Brazilian weathered lowland soil. Field Crop. Res. 218, 59–68. https://doi.org/10.1016/j.fcr.2018.01.002.

Borja Reis, A.F., Vasconcelos, A.L.S., Almeida, R.E.M., Lago, B.C., Dias, C.T.S., Favarin, J. L., 2018b. Relationship of nitrogen and crop performance in aerobic rice and continuous flooding irrigation in weathered tropical lowland. Eur. J. Agron. 95, 14–23. https://doi.org/10.1016/j.eja.2018.01.016.

Bouldin, D.R., 1986. The Chemistry and Biology of Flooded Soils in Relation to the Nitrogen Economy in Rice Fields. Nitrogen Economy of Flooded Rice Soils (S.K. De Datta and W.H. Patrick, Jr., eds.). Martinus Nijhoff Dordrecht 11–14.

Carracelas, G., Hornbuckle, J., Rosas, J., Roel, A., 2019. Irrigation management strategies to increase water productivity in Oryza sativa (rice) in Uruguay. Agric. Water Manag. 222, 161–172. https://doi.org/10.1016/j.agwat.2019.05.049.

Castañeda, A.R., Bouman, B.A.M., Peng, S., Visperas, R.M., 2002. The potential of aerobic rice to reduce water use in water-scarce irrigated lowlands in the tropics. In: Bouman B.A.M., Hengsdijk H., Hardy B., Bindraban P.S., Tuong T.P., Ladha, J.K. (Eds.), Water-wise Rice Production, Proceedings of the International Workshop on Water-wise Rice Production, Los Baños, Philippines, 8–11 April 2002, International Rice Research Institute, Los Baños, Philippines, 165–176.

Choudhury, B.U., Singh, A.K., 2016. Estimation of crop coefficient of irrigated transplanted puddled rice by field scale water balance in the semi-arid Indo-Gangetic Plains, India. Agric. Water Manag 176, 142–150. https://doi.org/10.1016/j.agwat.2016.05.027.

CONAB, 2022. Monitoring the Brazilian Grain Harvest 2021/2022. https://www.conab.gov.br/info-agro/safras/graos/boletim-da-safra-de-graos/item/download/41109_2a7211e86b7b0c1a6c2dba38abc9d97c. (Accessed 13 March 2022).

De Wit, A. 2022. Parameter sets for the WOFOST Crop Simulation Model. https://github.com/ajwdewit/WOFOST_crop_parameters (Accessed 16 March 2022).

De Wit, A., Boogaard, H., Fumagalli, D., Janssen, S., Knapen, R., Van Kraalingen, D., Supit, I., Van Der Wijngaart, R., Van Diepen, K., 2019. 25 years of the WOFOST cropping systems model. Agric. Syst. 168, 154–167. https://doi.org/10.1016/j.agsy.2018.06.018.

Dossou-Yovo, E.R., Saito, K., 2022. Impact of management practices on weed infestation, water productivity, rice yield and grain quality in irrigated systems in Côte d'Ivoire. Field Crop. Res. 270, 108209 https://doi.org/10.1016/j.fcr.2021.108209.

Durigon, A., Dos Santos, M.A., De Jong van Lier, Q., Metselaar, K., 2012. Pressure heads and simulated water uptake patterns for a severely stressed bean crop. Vadose Zone J. 11 (3). DOI:https://doi.org/10.2136/vzj2011.0187.

Embrapa - Brazilian Agricultural Research Corporation, 2008. Technical information for irrigated rice in the State of Tocantins. Embrapa Rice & Beans.

FAO, 2006. Guidelines for Soil Description, fourth ed. FAO, Rome, p. 95.

Feddes, R.A., Kowalik, E.J., Caradny, H., 1978. Simulation of Field Water Use and Crop Yield. Halstead Press, John Willey and Sons, New York, p. 188.

Gelsinari, S., Pauwels, V.R.N., Daly, E., Van Dam, J., Uijlenhoet, R., Fewster-Young, N., Doble, R., 2021. Unsaturated zone model complexity for the assimilation of evapotranspiration rates in groundwater modelling. Hydrol. Earth Syst. Sci. 25, 2261–2277. https://doi.org/10.5194/hess-25-2261-2021.

Groenendijk, P., Heinen, M., Klammler, G., Fankb, J., Kupfersberger, H., Pisinaras, V., Gemitzi, A., Peña-Harod, S., García-Prats, A., Pulido-Velazquez, M., Perego, A., Acutis, M., Trevisan, M., 2014. Performance assessment of nitrate leaching models for highly vulnerable soils used in low-input farming based on lysimeter data. Sci. Total Environ. 499, 463–480 https://doi.org/10.1016/j.scitotenv. 2014.07.002.

Hansen, S., Jensen, H.E., Nielsen, N.E., Svendsen, H., 1990. DAISY: soil plant atmosphere system model. NPO Report No. A 10. The National Agency for Environmental Protection, Copenhagen, p. 272.

IBGE - Brazilian Institute of Geography and Statistics, 2022. Automated recovery IBGE system–SIDRA. Municipal Agricultural Production. http://www.sidra.ibge.gov.br. (Accessed 7 April, 2022).

Ismail, H., Kamal, M.R., bin Abdullah, A.F., bin Mohd, M.S.F., 2020. Climate-smart agro-hydrological model for a large scale rice irrigation scheme in Malaysia. Appl. Sci. 10 (11), 3906. https://doi.org/10.3390/app10113906.

Kadiyala, M.D.M., Jones, J.W., Mylavarapu, R.S., Li, Y.C., Reddy, M.D., 2015. Identifying irrigation and nitrogen best management practices for aerobic rice–maize cropping system for semi-arid tropics using CERES-rice and maize models. Agric. Water Manag. 149, 23–32. https://doi.org/10.1016/j.agwat.2014.10.019.

Kroes, J.G., Van Dam, J.C., Bartholomeus, R.P., Groenendijk, P., Heinen, M., Hendriks, R. F.A., Mulder, H.M., Supit, I., Van Walsum, P.E.V., 2017. SWAP version 4; Theory Description and User Manual.

Kroes, J., van Dam, J., Supit, I., de Abelleyra, D., Ver´on, S., de Wit, A., Boogaard, H., Angelini, M., Damiano, F., Groenendijk, P., Wesseling, J., Veldhuizen, A., 2019. Agrohydrological analysis of groundwater recharge and land use changes in the Pampas of Argentina. Agric. Water Manag. 213, 843–857 https://doi.org/10.1016/j.agwat.2018.12.008.

Kukal, S.S., Hira, G.S., Sidhu, A.S., 2005. Soil matric potential-based irrigation scheduling to rice (Oryza sativa). Irrig. Sci. 23, 153–159. https://doi.org/10.1007/s00271-005-0103-8.

LaHue, G.T., Linquist, B.A., 2019. The magnitude and variability of lateral seepage in California rice fields. J. Hydrol. 574, 202–2010. https://doi.org/10.1016/j.jhydrol.2019.04.030.

LaHue, G.T., Linquist, B.A., 2021. The contribution of percolation to water balances in water-seeded rice systems. Agric. Water Manag. 243, 106445 https://doi.org/10.1016/j.agwat.2020.106445.

Mainuddin, M., Maniruzzaman, M., Alam, M.M., Mojid, M.A., Schmidt, E.J., Islam, M.T., Scobie, M., 2020. Water usage and productivity of Boro rice at the field level and their impacts on the sustainable groundwater irrigation in the North-West Bangladesh. Agric. Water Manag. 240, 106294 https://doi.org/10.1016/j.agwat.2020.106294.

Melo, M.L.A., De Jong van Lier, Q., 2021. Revisiting the Feddes reduction function for modeling root water uptake and crop transpiration. J. Hydrol. 603 (Part B), 126952 https://doi.org/10.1016/j.jhydrol.2021.126952.

Monteith, J.L., 1981. Evaporation and surface temperature. Q. J. R. Meteorol. Soc. 107, 1–24.
Mualem, Y., 1976. A new model for predicting the hydraulic conductivity of unsaturated porous media. Water Resour. Res. 12 (3), 513–522. https://doi.org/10.1029/WR012i003p00513.
Perry, H., Carrijo, D., Linquist, B., 2022. Single midseason drainage events decrease global warming potential without sacrificing grain yield in flooded rice systems. Field Crop. Res. 276, 108312 https://doi.org/10.1016/j.fcr.2021.108312.
Pinheiro, E.A.R., De Jong van Lier, Q., 2021. Propagation of uncertainty of soil hydraulic parameterization in the prediction of water balance components: a stochastic analysis in kaolinitic clay soils. Geoderma 388, 114910. https://doi.org/10.1016/j.geoderma.2020.114910.
Pinheiro, E.A.R., De Jong van Lier, Q., Šimůnek, J., 2019. The role of soil hydraulic properties in crop water use efficiency: a process-based analysis for some Brazilian scenarios. Agric. Syst. 173, 364–377. https://doi.org/10.1016/j.agsy.2019.03.019.
Pinheiro, E.A.R., Metselaar, K., van Lier, Q.J., de Araújo, J.C., 2016. Importance of soil-water to the Caatinga biome, Brazil. Ecohydrology 9, 1313–1327. https://doi.org/10.1002/eco.1728.
Santos, C.L., Borja Reis, A.F., Mazzafera, P., Favarin, J.L., 2018a. Determination of the water potential threshold at which rice growth is impacted. Plants 7 (3), 48. DOI: https://doi.org/10.3390/plants703004.
Santos, H.G., Lumbreras, J.F., Coelho, M.R., Araujo Filho, J.C., Cunha, T.J.F., Jacomine, P.K.T., Anjos, L.H.C., Oliveira, V.A., Almeida, J.A., Oliveira, J.B., 2018b. National Soils Research Center Manual of Soil Analysis Methods, fifth ed., Embrapa Soils, Brasilia-DF.
Šimůnek, J., Van Genuchten, M., Th, Šejna, M., 2008. Development and applications of the HYDRUS and STANMOD software packages and related codes. Vadose Zone J. 7, 587–600. https://doi.org/10.2136/vzj2007.0077.
Singh, J., Ge, Y., Heeren, D.M., Bai, G., Neale, C.M.U., Woldt W.E., 2021. Sensor-Based Irrigation of Maize and Soybean in East-Central Nebraska under a Sub-Humid Climate – ASABE 2021. In: Proceedings of the Annual International Meeting Paper. DOI:doi.org/10.13031/aim.21001044.
Singh, R., Van Dam, J.C., Feddes, R.A., 2006. Water productivity analysis of irrigated crops in Sirsa district, India. Agric. Water Manag. 82 (3), 253–278. https://doi.org/10.1016/j.agwat.2005.07.027.
SOSBAI, South Brazilian Irrigated Rice Society, 2018. Irrigated rice: technical research recommendations for Southern Brazil. Porto Alegre 205.
Taufik, M., Setiawan, B.I., Van Lanen, H.A.J., 2018. Increased fire hazard in human-modified wetlands in Southeast Asia. Ambio 48, 363–373. https://doi.org/10.1007/s13280-018-1082-3.
Tong, Y.D., 2017. Rice intensive cropping and balanced cropping in the Mekong Delta, Vietnam — economic and ecological considerations. Ecol. Econ. 132, 205–212. https://doi.org/10.1016/j.ecolecon.2016.10.013.
Tuong, T.P., Bouman, B.A.M., 2003. Rice production in water-scarce environments. In: Kijne, J.W., Barker, R., Molden, D. (Eds.), Water Productivity in Agriculture: Limits and Opportunities for Improvement. CABI Publishing, pp. 53–67.
Turek, M.E., van Lier, de Jong, Armindo, R.A, Q., 2020. Estimation and mapping of field capacity in Brazilian soils. Geoderma 376, 114557. https://doi.org/10.1016/j.geoderma.2020.114557.
Van Dam, J.C., Feddes, R.A., 2000. Numerical simulation of infiltration, evaporation and shallow groundwater levels with the Richards equation. J. Hydrol. 233, 72–85. https://doi.org/10.1016/S0022-1694(00)00227-4.
Van Genuchten, M.Th, 1980. A closed form equation for predicting the hydraulic conductivity of unsaturated soils. Soil Sci. Soc. Am. J. 44, 892–898.
Van Genuchten, M.Th., Leij, F.J., Yates, S.R., 1991. The RETC Code for Quantifying the Hydraulic Functions of Unsaturated Soils, Version 1.0. EPA Report 600/2-91/065, U. S. Salinity Laboratory, USDA, ARS, Riverside, CA.
Vazifedoust, M., Van Dam, J.C., Feddes, R.A., Feizi, M., 2008. Increasing water productivity of irrigated crops under limited water supply at field scale. Agric. Water Manag. 95 (2), 89–102. https://doi.org/10.1016/j.agwat.2007.09.007.
Wang, H., Zhang, Y., Zhang, Y., McDaniel, M.D., Sun, L., Su, W., Fan, X., Liu, S., Xiao, X., 2020. Water-saving irrigation is a 'win-win' management strategy in rice paddies – With both reduced greenhouse gas emissions and enhanced water use efficiency. Agric. Water Manag. 228, 105889 https://doi.org/10.1016/j.agwat.2019. 105889.
Yamaguchi, T., Tuan, L.M., Minamikawa, K., Yokoyama, S., 2019. Assessment of the relationship between adoption of a knowledge-intensive water-saving technique and irrigation conditions in the Mekong Delta of Vietnam. Agric. Water Manag. 212, 162–171. https://doi.org/10.1016/j.agwat.2018.08.041.
Yuan, C., Feng, S., Huo, Z., Ji, Q., 2019. Simulation of saline water irrigation for seed maize in arid northwest China based on SWAP model. Sustainability 11 (16), 4264. https://doi.org/10.3390/su11164264.
Zhuang, Y., Zhang, L., Li, S., Liu, H., Zhai, L., Zhou, F., Ye, Y., Ruan, S., Wen, W., 2019. Effects and potential of water-saving irrigation for rice production in China. Agric. Water Manag. 217, 374–382. https://doi.org/10.1016/j.agwat.2019.03.010.
Zwart, S.J., Bastiaanssen, W.G.M., 2004. Review of measured crop water productivity values for irrigates wheat, rice, cotton and maize. Agric. Water Manag. 69, 115–133. https://doi.org/10.1016/j.agwat.2004.04.007.